Density Functional Calculations of ^{95}Mo NMR Chemical Shifts: Applications to Model Catalysts for Imine Metathesis

Michael Bühl[a]

Dedicated to Prof. Dr. Wolfgang von Philipsborn on the occasion of his 70th birthday

Abstract: Nonlocal density functional theory is used to the compute geometries and ^{95}Mo chemical shifts of MoO_4^{2-}, MoO_3S^{2-}, $MoO_2S_2^{2-}$, $MoOS_3^{2-}$, MoS_4^{2-}, $MoSe_4^{2-}$, $[Mo(CO)_6]$, $[Mo(C_5H_5)(CO)_3H]$, $[Mo(C_6H_6)_2]$, $[Mo_2(OMe)_6]$, and $[Mo_2(O_2CH)_4]$. For this set of compounds, the effect of the substituents on $\delta(^{95}Mo)$ are described well by pure density functionals; however, they are significantly overestimated with the B3LYP hybrid functional. With the latter, ^{95}Mo chemical shifts of systems with Mo–Mo multiple bonds show additional large errors. $\delta(^{95}Mo)$ values between -521 and $+89$ are predicted for $[Mo(NH)_2X_2]$ (X = F, Cl, Br, OMe, OCF_3), which are model compounds for imine-metathesis catalysts. The mechanism of imine metathesis with these model catalysts is studied, and the key step is indicated to be the reversible formation of a diazametallacycle from the initial $[Mo(NH)_2X_2(NH{=}CH_2)]$ adduct. This process can occur via two distinct transition states which have different stereochemistry. For various X, the $\delta(^{95}Mo)$ values of the reactants (or OMe_2 adducts thereof) are loosely correlated with the higher of these two barriers; however, not with the lower, rate-determining one. Thus, no general correlation between $\delta(^{95}Mo)$ and catalytic activities should be expected for the real imine-metathesis catalysts. From the loose correlation with the higher barrier, however, one might speculate that complexes with particularly shielded ^{95}Mo nuclei may be more active catalysts, which would allow the selection of suitable target complexes based on $\delta(^{95}Mo)$ data from the literature.

Keywords: density functional calculations · homogeneous catalysis · metathesis · NMR spectroscopy · reaction mechanisms

Introduction

Transition metal NMR spectroscopy is especially useful when it can serve as a probe for reactivity.[1] Numerous systems that contain transition metals are known in which the NMR properties of the metal atom, usually the chemical shifts, can be correlated with rate constants[2] or with catalytic activities.[3] Modern theoretical methods based on density functional theory (DFT) can be used to reproduce and rationalize such relationships[4] or to predict new ones.[5] The great potential of such correlations is that, once established, they allow the reactivity or catalytic activity of a newly synthesized derivative to be estimated from its NMR spectrum.

For a given reaction, the theoretical approach involves the identification of the rate-determining step, followed by investigations of how variations in the ligand sphere affect the corresponding barrier and the value of the chemical shift for the metal in the reactant complex. DFT is now well established as a tool to reliably compute geometries and energetics,[6] as well as NMR properties,[7] of transition metal complexes.

The recently discovered catalysis of imine metathesis by imido molybdenum complexes[8] (Scheme 1) would be an attractive candidate to study the correlation between the NMR data and the reactivity. Mo complexes are widely used in homogeneous catalysis; the most important area is probably olefin metathesis by alkylidene derivatives. This reaction has been well studied, both experimentally[9] and theoretically,[10] and the key step involves the reversible formation of a four-membered metallacycle. Very efficient and versatile catalysts have been developed which leave little room for improvement.

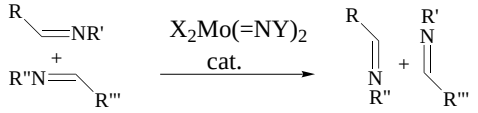

Scheme 1. The catalysis of imine metathesis by imido molybdenum complexes.

[a] Dr. M. Bühl[+]
Organisch-chemisches Institut, Universität Zürich
Winterthurerstrasse 190, CH-8057 Zürich (Switzerland)

[+] Present address:
Max-Planck-Institut für Kohlenforschung
Kaiser-Wilhelm-Platz 1, D-45470 Mülheim/Ruhr (Germany)
Fax: (+49)208-306-2996
E-mail: buehl@mpi-muelheim.mgp.de

Supporting information for this article is available on the WWW under http://www.wiley-vch.de/home/chemistry/ or from the author.

0947-6539/99/0512-3514 $ 17.50+.50/0

Compared to olefin metathesis, the analogous reaction involving imines requires more drastic conditions, that is higher temperatures and longer reaction times. In order to design more active catalysts, a detailed knowledge of the underlying mechanism would be desirable. A density functional study is thus presented for a suitable model system, calling special attention to on substituent effects on energetics and ^{95}Mo chemical shifts. If a correlation between the $\delta(^{95}\mathrm{Mo})$ values and key barriers of the imido complexes could be predicted, it might be possible to devise modifications—for instance, based on NMR data from the literature—in order to increase the activity of the actual catalysts. Interesting strereoelectronic effects of substituents are found in the key transition structures in the model reaction; however, it is unfortunate that no general correlation between the NMR data and the reactivity can be predicted.

The chemical shifts of the metal nuclei themselves remain a challenge insofar as the results can be very sensitive to the particular density functional employed. In the cases studied hitherto, hybrid functionals, such as the popular B3LYP combination, have proven to be superior to "pure" density functionals, particularly for the chemical shifts of ^{57}Fe,[11] ^{103}Rh,[11] and ^{59}Co.[12] In order to test the generality of these performances, a systematic study of ^{95}Mo chemical shifts is included in the present paper.[13] This nucleus is one of the more readily accessible ones among the transition metals, and a sizable amount of experimental data is known.[14] As it turns out, the pure density functionals provide the best $\delta(^{95}\mathrm{Mo})$ values, whereas B3LYP can lead to large errors in specific cases.

The objectives of this paper are thus twofold: Firstly, to identify the density functionals that provide the best performance in ^{95}Mo chemical-shift computations, and secondly, to study substituent effects on $\delta(^{95}\mathrm{Mo})$ values and rate-determining barriers for an imine-metathesis model system.

Abstract in German: *Die Geometrien und ^{95}Mo chemischen Verschiebungen von MoO_4^{2-}, MoO_3S^{2-}, $MoO_2S_2^{2-}$, $MoOS_3^{2-}$, MoS_4^{2-}, $MoSe_4^{2-}$, $[Mo(CO)_6]$, $[Mo(C_5H_5)(CO)_3H]$, $[Mo(C_6H_6)_2]$, $[Mo_2(OMe)_6]$ und $[Mo_2(O_2CH)_4]$ wurden mittels Dichtefunktionaltheorie in nichtlokaler Näherung berechnet. Für diese Verbindungen werden Substituenteneffekte auf $\delta(^{95}\mathrm{Mo})$ gut mit "reinen" Dichtefunktionalen beschrieben, mit dem B3LYP-Hybridfunktional dagegen deutlich überschätzt. Mit letzterem ergeben sich zusätzlich große Fehler für die ^{95}Mo chemischen Verschiebungen in Systemen mit Mo–Mo-Mehrfachbindungen. $\delta(^{95}\mathrm{Mo})$-Werte zwischen $\delta = -521$ und $+89$ werden für $[Mo(NH)_2X_2]$ vorhergesagt ($X = F$, Cl, Br, OMe, OCF_3), welche als Modellverbindungen für Iminmetathese-Katalysatoren dienen. Die Untersuchung des Mechanismus der Iminmetathese mit diesen Modell-Katalysatoren legt als Schlüsselschritt die reversible Bildung eines Diazametallazyklus aus einem primär gebildeten $[Mo(NH)_2X_2(NH{=}CH_2)]$ Addukt nahe. Dieser Prozeß kann über zwei verschiedene Übergangszustände mit unterschiedlicher Stereochemie verlaufen. Bei Variation der Substituenten X korrelieren die $\delta(^{95}\mathrm{Mo})$-Werte der Edukte (oder deren OMe_2-Addukte) lose mit der höheren der beiden Barrieren, nicht jedoch mit der niedrigeren, geschwindigkeitsbestimmenden. Daher sollte man für die realen Iminmetathese-Katalysatoren keine generelle Korrelation zwischen $\delta(^{95}\mathrm{Mo})$ und katalytischer Aktivität erwarten. Aufgrund der losen Korrelation mit der höheren Barriere kann man jedoch spekulieren, daß Komplexe mit besonders stark abgeschirmtem ^{95}Mo-Kern eine erhöhte katalytische Aktivität aufweisen könnten, was die Auswahl geeigneter Zielmoleküle anhand von $\delta(^{95}\mathrm{Mo})$-Daten aus der Literatur erlauben würde.*

Computational Details

Methods and basis sets correspond to those used in the previous studies of rhodium complexes, namely the geometries have been fully optimized in the given symmetry at the BP86/ECP1 level, by the use of the exchange and correlation functionals of Becke[15] and Perdew,[16] respectively, together with a fine integration grid (75 radial shells with 302 angular points per shell), a relativistic MEFIT effective core potential with the corresponding [6s5p3d] valence basis set for Mo,[17] and the standard 6-31G* basis set[18, 19] for all other elements. For the model compounds with Cl substituents for the metathesis reaction, the nature of the stationary points has been verified by calculations of harmonic vibrational frequencies (by means of numerical differentiation of the analytical first derivatives), from which the zero-point energies (ZPEs) have also been obtained. Geometries and energies (including ZPEs where available) are provided in the Supporting Information in the form of Gaussian archive entries.

Magnetic shieldings have been evaluated for the BP86/ECP1 geometries by the use of a recent implementation of the GIAO (gauge-including atomic orbitals) method,[20] both at the Hartree–Fock (HF) and the DFT levels, whereby the latter involves the functional combinations according to Becke[15] and to Perdew and Wang[21] (denoted BPW91) or Becke (hybrid)[22] and Lee, Yang, and Parr,[23] (denoted B3LYP), together with basis II, that is a [16s10p9d] all-electron basis for Mo, contracted from the well-tempered 22s14p12d set of Huzinaga and Klobukowski[24] and augmented with two d-shells of the well-tempered series, and the recommended IGLO-basis II[25, 26] on all other atoms. In addition, magnetic shieldings have been computed with the UDFT-IGLO (uncoupled DFT with individual gauge for localized orbitals) and the SOS-DFPT-IGLO (sum-over-states density-functional perturbation theory) method in its LOC1 approximation.[27] Chemical shifts are reported in ppm relative to MoO_4^{2-} (**1**), the experimental standard (absolute shieldings -1729, -1358, -1196, -1192, and -1113 ppm at GIAO-HF, GIAO-B3LYP, GIAO-BPW91, UDFT-IGLO and SOS-DFPT-IGLO levels, respectively). All computations employed the Gaussian 94 program package,[28] except for the UDFT-IGLO and SOS-DFPT-IGLO calculations which used the implementation in the deMon code.[29]

Results and Discussion

This section is organized as follows: firstly, a systematic DFT study of ^{95}Mo chemical shifts is presented in order to identify the density functionals best suited to the computation of this property. Secondly, the model reaction for imine metathesis is investigated in terms of key intermediates and transition structures, and includes an assessment of substituent effects on the rate-determining barrier and on $\delta(^{95}\mathrm{Mo})$ of the reactants.

Geometries and chemical shifts: Optimized geometries for the test set **1**–**11**, which comprises both inorganic and organometallic species, are displayed in Figure 1, together with key geometrical parameters. Available distances ob-

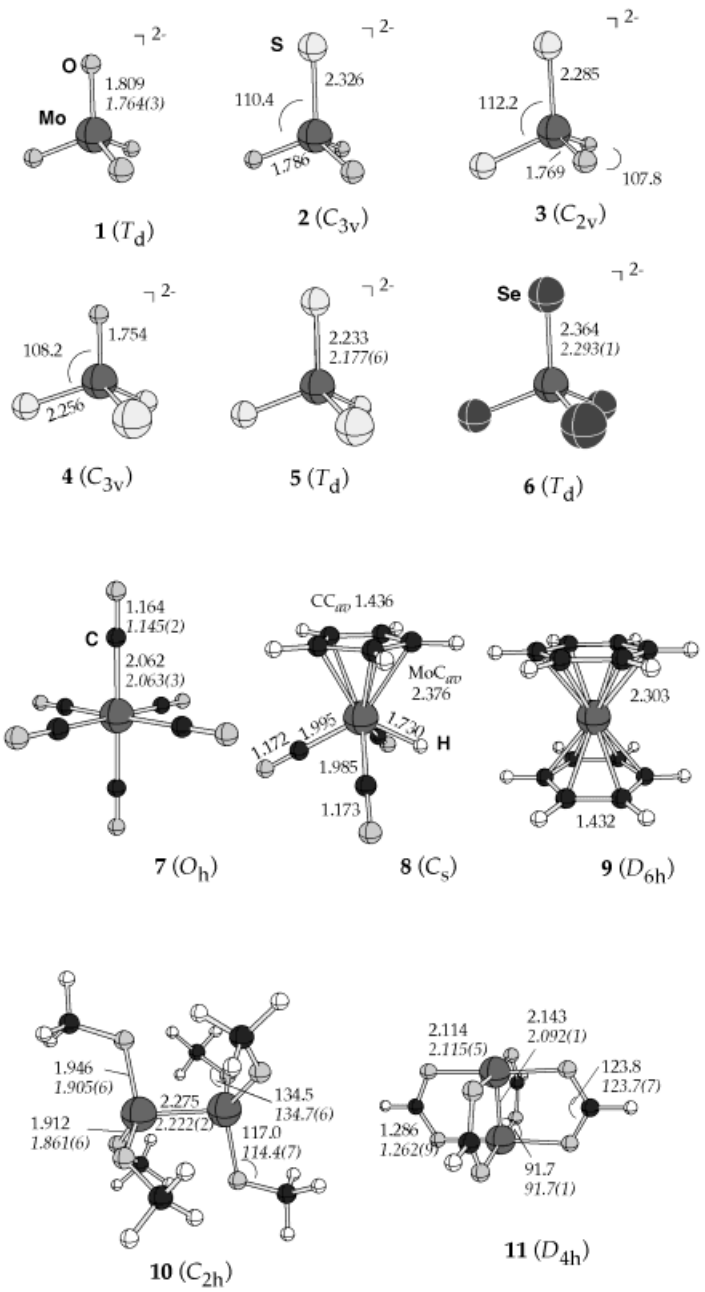

Figure 1. BP86/ECP1-optimized geometries including key geometrical parameters [Å and °], together with the corresponding averaged experimental data, where available (in italics).[30–32] The compounds are MoO_4^{2-}(**1**), $MoSO_3^{2-}$(**2**), $MoS_2O_2^{2-}$(**3**), MoS_3O^{2-}(**4**), MoS_4^{2-}(**5**), $MoSe_4^{2-}$(**6**), $[Mo(CO)_6]$ (**7**), $[Mo(C_5H_5)(CO)_3H]$ (**8**), $[Mo(C_6H_6)_2]$ (**9**), $[Mo_2(OMe)_6]$ (**10**), and $[Mo_2(O_2CH)_4]$ (**11**).

served in the solid state for **1**, **5**, **6**, and **11** are included for comparison,[30] as are structural data for $[Mo_2(OCH_2CMe_3)_6]$[31] for which **10** serves as model, as well as the gas-phase electron-diffraction (GED) results for **7**,[32] the only known gas-phase structure in this set.[33] As noted before for these or for similar compounds,[6] bond lengths between the transition metal and the main-group elements tend to be overestimated by up to several pm at the DFT level employed— even more so for the inorganic dianions than for the organometallic species.[34, 35] The Mo–Mo triple and quadruple bond lengths in **10** and **11**, respectively, are reasonably well described at the BP86/ECP1 level.

Relative ^{95}Mo chemical shifts, computed at the UDFT-IGLO and SOS-DFPT-IGLO, GIAO-HF, GIAO-BPW91, and GIAO-B3LYP levels are summarized in Table 1. The latter two $\delta(^{95}Mo)$ sets are plotted versus the experimental values in Figure 2. The best agreement with experimental values is obtained at the GIAO-BPW91 level, as evidenced by the near-ideal gradient of the δ_{calc} versus δ_{exp} linear regression, 1.01, and by the relatively small mean absolute deviation, 245 ppm (Table 1, Figure 2a). The latter mean error is quite satisfactory when compared to the covered range of ^{95}Mo chemical shifts, more than 5500 ppm. In addition, the deviation is quite systematic: most of the computed δ values exhibit too strong a deshielding with respect to experiment. The performance of SOS-DFPT,[36] UDFT-IGLO and GIAO-BPW91 is quite similar, whereby UDFT-IGLO affords a somewhat smaller mean average error, but a larger slope than the other two methods (Table 1).

Large deviations between the computed and the experimental δ values are found at the GIAO-HF level, manifested in a significant overestimation of the range of chemical shifts (Table 1). The analysis of the GIAO-HF σ values reveals almost constant diamagnetic contributions, σ_d (very similar to those obtained at the DFT levels), and the deviations of the δ values can be traced back to a strong overestimation of the paramagnetic contributions, σ_p. The molybdate derivatives **1**–**6** have been the subject of previous studies at the HF level which employed finite perturbation theory (FPT)[37] and the localized-orbitals-local-origin (LORG) approach.[38] While excellent agreement with the experimental values was found in the former study, the latter work revealed similar overestimations of the δ values, as found here. Apparently, the degree of accuracy of the FPT data is largely an artifact of the small basis sets employed, and the suggestion in ref. [38] regarding the presumed importance of electron-correlation effects is correct (since inclusion of these effects at the DFT levels reduces the errors of GIAO-HF).[39]

For Mo–Mo systems **10** and **11** with Mo–Mo multiple bonds, GIAO-HF fails completely, as excessively large σ values are computed (exceeding 10000 ppm). It is well known that a single-reference HF wavefunction cannot describe multiple bonds between transition metals correctly,[40] which, apparently, leads to the spectacular errors in σ_p.

For the transition metal nuclei studied so far, inclusion of the HF exchange in the so-called hybrid functionals, such as B3LYP, has resulted in a proportional increase of the paramagnetic contribution, σ_p, and thus in more deshielded δ values.[5, 7b, 11] The same is found for the ^{95}Mo chemical shifts in Table 1. Since the "pure DFT" results (UDFT-IGLO, SOS-DFPT and GIAO-BPW91) are already in good agreement with experimental values, the corresponding B3LYP values tend to be too strongly deshielded, which leads to a much larger $\delta_{calcd}/\delta_{exp}$ slope (1.27) and a much larger mean absolute deviation (416 ppm). Additional shortcomings are apparent for **10** and **11** which deviate notably from the $\delta_{calcd}/\delta_{exp}$ correlation (Figure 2b), to produce errors of up to ≈1800 ppm with respect to experiment (for **11**). These errors are probably related to the above-mentioned

0947-6539/99/0512-3516 $ 17.50+.50/0 *Chem. Eur. J.* **1999**, *5*, No. 12

Table 1. Theoretical ^{95}Mo chemical shifts in complexes **1**–**11**, δ relative to **1**.[a]

Molecule	GIAO-HF	GIAO-B3LYP	SOS-DFPT-IGLO	UDFT-IGLO	GIAO-BPW91	Expt.[b]
MoO_4^{2-}(**1**)	0	0	0	0	0	0
$MoSO_3^{2-}$(**2**)	800	479	424	438	399	497
$MoS_2O_2^{2-}$(**3**)	1945	1091	923	966	902	1067
MoS_3O^{2-}(**4**)	3401	1765	1481	1560	1451	1654
MoS_4^{2-}(**5**)	5079	2515	2076	2174	2056	2259
$MoSe_4^{2-}$(**6**)	8434	3668	2885	3015	2929	3145
$[Mo(CO)_6]$ (**7**)	−2479	−2350	−2319	−3015	−2294	−1856
$[Mo(C_5H_5)(CO)_3H]$ (**8**)	−2232	−2413	−2365	−2387	−2422	−2047
$[Mo(C_6H_6)_2]$ (**9**)	−1148	−1518	−1875	−1813	−1698	−1362
$[Mo_2(OMe)_6]$ (**10**)	–[c]	3273	2196	2236	2174	2447[d]
$[Mo_2(O_2CH)_4]$ (**11**)	–[c]	5517	3216	3374	3311	3702[e]
slope[f]	(1.89)	1.27	1.02	1.05	1.01	
mean absolute deviation from experiment	(1340)	416	260	209	245	

[a] Basis II and BP86/ECP1 geometries employed. [b] From ref. [14]. [c] Unreasonably large numbers obtained. [d] Experimental value for $[Mo_2(OCH_2tBu)_6]$. [e] Experimental value for $[Mo_2(O_2CMe)_4]$. [f] Slope of the linear regression for δ_{calcd} versus δ_{expt}.

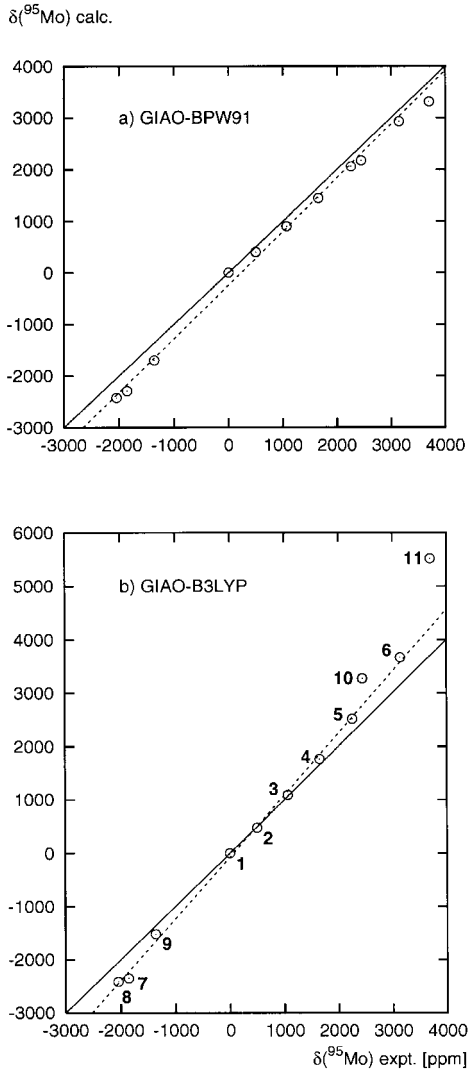

Figure 2. Plot of computed (basis II for BP86/ECP1-optimized geometries) versus the experimental ^{95}Mo chemical shifts. a) GIAO-BPW91 level, b) GIAO-B3LYP level. Linear regression lines (dashed) and ideal lines with the slope 1 (solid) are included.

failure of the HF method for these compounds.[41] Care should thus be taken when studying metal–metal multiple bonds with the popular B3LYP approach.

Therefore, in contrast with theoretical transition metal chemical shifts investigated so far, the performance of the GIAO-B3LYP method is noticeably worse for $\delta(^{95}Mo)$ values than that of pure DFT approaches.[42] In the case of systems with Mo–Mo multiple bonds, the complete failure of the HF method also causes the B3LYP chemical shifts to deteriorate considerably. In summary, the GIAO-B3LYP method cannot be recommended for ^{95}Mo chemical shifts so that, in the following, results are reported at the GIAO-BPW91 level. B3LYP is thus not a panacea and one is left with the somewhat unsatisfactory conclusion that for computations of transition metal chemical shifts, the various functionals have to be carefully reassessed for each new problem at hand. While this situation calls for new and improved density functionals,[43] it should not prevent selected applications of such calculations, as illustrated in the second part of this paper.

Imine metathesis

Mechanism: The reaction of $H_2C{=}NH$ with $[Mo(NH)_2Cl_2]$ (**12**) will now be discussed as a model for imine metathesis (Scheme 1). Corresponding model studies for the key step in olefin metathesis (Scheme 2, X = Cl, Y = NH, R = H) have

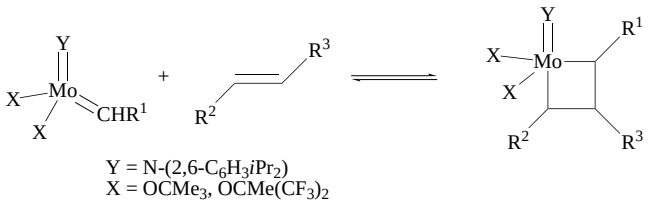

Scheme 2. The key step in the olefin metathesis reaction.

indicated small barriers for the addition of ethylene to Mo-alkylidene complexes, for example, $\approx$10 kJ mol^{-1} for $[Mo(O)(CH_2)Cl_2]$, and a substantial energetic driving force for the formation of the metallacyclobutane of 38–74 kJ mol^{-1}[10b] (66.5 kJ mol^{-1} for $[Mo(NH)(CH_2)Cl_2]$ + ethylene at the BP86/ECP1 + ZPE level). For this simple model reaction, in the absence of entropy effects, the metallacyclobutane would be the resting state of the catalyst, while its decomposition (reverse reaction in Scheme 2) would be the

rate-determining step. Entropy strongly disfavors the metallacycle and the free energy necessary for its decay is computed to be very small at ambient temperature (18.0 kJ mol^{-1} for [Mo(NH)(*c*-C_3H_6)Cl_2], BP86/ECP1 level), consistent with the observed high activities of the alkylidene catalysts.

The analogous diazametallacyclobutanes have been proposed as possible intermediates in the catalytic cycle for imine metathesis[8c] (**A** in Scheme 3). In addition, there is spectroscopic evidence for the formation of complexes with a coordinated imine which have been suggested as further intermediates in the cycle (**B** in Scheme 3).[8c] The corresponding minima and key transition structures have been located for the model reaction and are presented in Figure 3.

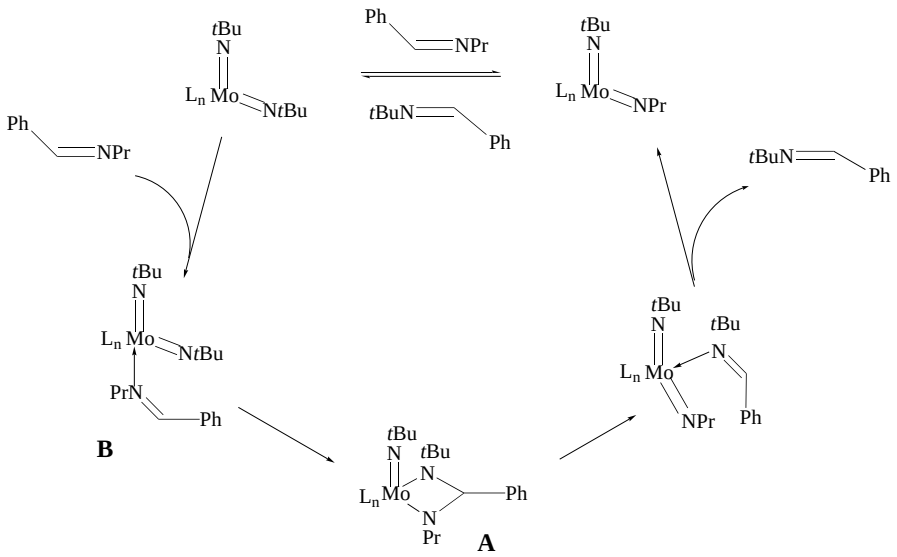

Scheme 3. Proposed mechanism of the catalytic cycle for imine metathesis.

The parent diazametallacycle **14** indeed proved to be a minimum on the potential energy surface (PES). While the carbon analogue, [Mo(NH)(*c*-C_3H_6)Cl_2], can adopt two coordination geometries, square pyramidal (sp) and, slightly higher in energy, trigonal bipyramidal (tbp),[10b,c] only one isomer could be located for **14**, which is more reminiscent of a tbp arrangement (with the imido and one of the amido ligands in the axial positions). Formation of **14** from **12** + H_2C=NH is computed to be exothermic by −65.7 kJ mol^{-1} on the PES (BP86/ECP1 level, −49.4 kJ mol^{-1} including ZPE) and almost thermoneutral on the free energy surface (−1.2 kJ mol^{-1}); the diazametallacycle may thus be a viable intermediate. Related thiourea derivatives are known, for instance [Mo(NAr){N(Ph)C(=S)N(Ar)}(O*t*Bu)$_2$] (Ar = 2,6-*i*PrC_6H_3),[44] which, in the solid state, adopts a conformation similar to that of **14**.

Intermediate **14** is not formed in a single step from the reactants: even when the imine is placed side-on to the Mo center of **12** (in search of a possible π complex), the optimization leads to a Lewis base complex in which the imine is coordinated through its nitrogen lone pair, consistent

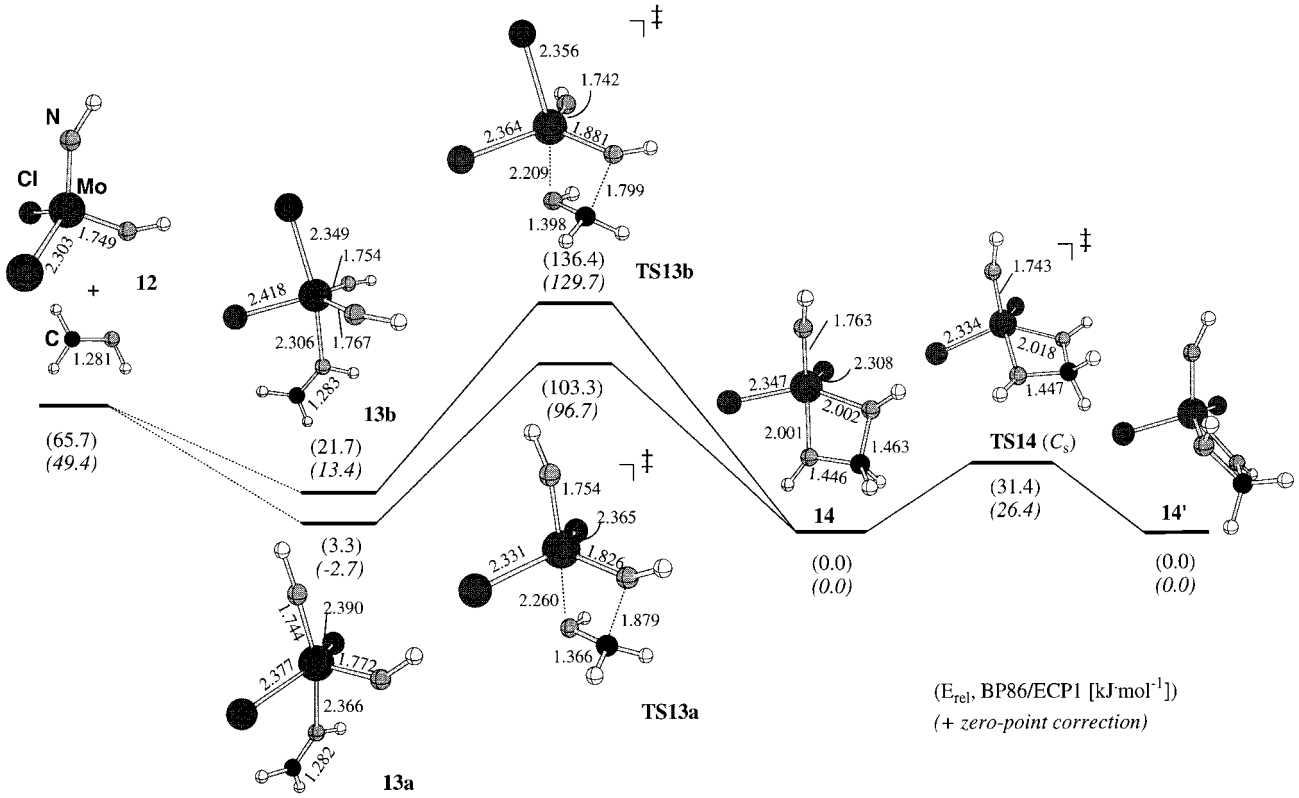

Figure 3. Schematic reaction profile for the addition of H_2C=NH to **12** (BP86/ECP1 level).

0947-6539/99/0512-3518 $ 17.50+.50/0 *Chem. Eur. J.* **1999**, *5*, No. 12

with the observation of the corresponding intermediates **B** (Scheme 3).[8c] Two Lewis complexes have been located, **13b** and **13a** (Figure 3), where coordination occurs *trans* to a chloro and an imido ligand, respectively, with the latter being somewhat more stable (by $\approx$16 kJ mol^{-1} at BP86/ECP1 + ZPE).

Both Lewis complexes can rearrange to the metallacycle **14** via transition structures **TS13b** and **TS13a**, respectively (Figure 3). In these structures, the CH_2 group has migrated towards the imido moiety and the free lone pair has reappeared at the incoming nitrogen (as apparent from the degree of pyrimidalization).[45] In **TS13b** and **TS13a**, this incoming nitrogen remains *trans* to Cl and *trans* to NH, respectively. As in **13b** and **13a**, the arrangement with imido and incoming imino ligands *trans* to each other is more favorable; the energetic separation is even larger in the transition states, and **TS13b** is computed to be higher than **TS13a** by 38 kJ mol^{-1}. There is thus a large stereoelectronic effect in the transition state (see below).

The two nitrogen atoms in the four-membered ring of **14** are not equivalent as a result of the lack of symmetry. For metathesis, the scrambling of these two nitrogen atoms has to occur. In the model reaction studied here, this scrambling can be achieved via the C_s-symmetric **TS14** which has a square-pyramidal ligand arrangement about Mo (Figure 3; **14′** is the mirror image of **14**). The barrier computed for this process is quite low, no larger than 26.4 kJ mol^{-1} (this value is actually an upper limit since **TS14** has two imaginary frequencies and is thus a second-order saddle point; the true transition structure has not been located). The barriers for formation and decomposition of the metallacycle are much higher, nearly 100 kJ mol^{-1} (via **TS13a**), and should thus be rate-determining. A similar barrier, 88.2 kJ mol^{-1}, has recently been computed for the addition of ethylene to the imido group of $[MoO(NH)Cl_2]$.[46] These barriers are much higher than those involved in olefin metathesis with alkylidene complexes (see above), which is consistent with the more drastic reaction conditions necessary for imine metathesis. Under these reaction conditions, however, barriers in the order of 100 kJ mol^{-1} are not insurmountable and the mechanism illustrated in Figure 3 represents a viable pathway for imine metathesis, and supports the proposition that diazametallacyles and labile imine adducts are involved (**A** and **B**, respectively, in Scheme 2).

Table 2. Computed (BPW91/II) properties of complexes $[Mo(NH)_2X_2]$.[a]

X	δ	(δ OMe_2)	q(Mo)[b]	Σd(Mo)[b,c]	$\sigma_p^{k\rightarrow a}$[d, e]	$\Delta\varepsilon$ [eV][e]
Br (**15**)	93	(289)	0.84	4.85	−3137	5.49
Cl (**12**)	−89	(116)	0.94	4.77	−2788	6.01
OMe (**16**)	−296	(−26)	1.33	4.50	−762	9.05
OCF_3 (**17**)	−438	(−235)	1.31	4.51	−233	10.47
F (**18**)	−521	(−312)	1.45	4.38	−1490	8.08

[a] ^{95}Mo chemical shifts δ (GIAO method, in parentheses: δ of OMe_2 adducts), natural charges q(Mo), d-orbital populations d(Mo), and contribution to σ_P and energy difference $\Delta\varepsilon$ of the key orbitals sketched in Figure 4. [b] From natural population analyses. [c] Sum of the 4d populations on Mo. [d] Contribution to the paramagnetic part of the shielding tensor in x direction (in ppm), arising from the coupling of pairs of occupied and virtual MOs that correspond to those of Figure 4; the virtual MO is the LUMO in all cases, occupied MOs are $16b_1$, 15b, 23b, and $7b_1$ for **15**, **16**, **17**, and **18**, respectively. [e] UDFT with common gauge origin at the metal.

relevant data for the model species $[Mo(NH)_2X_2]$ (X = Br,[47] Cl, OMe, OCF_3, and F). In this series, the ^{95}Mo nucleus is computed to be increasingly shielded, despite the increasing electron-withdrawing capability of the substituents. Results from natural population analysis (NPA)[48] in Table 3 confirm that the electronic charge is indeed increasingly withdrawn from Mo in this series: total positive charge and d-orbital population increase and decrease, respectively.

In this model system, it appears to be the energetic separation between occupied and virtual orbitals of suitable symmetry which is decisive and which is subject to modification by the substituents. Analysis of the many individual MO contributions is difficult; however, the discussion of a particular example can be instructive: Figure 4 shows a

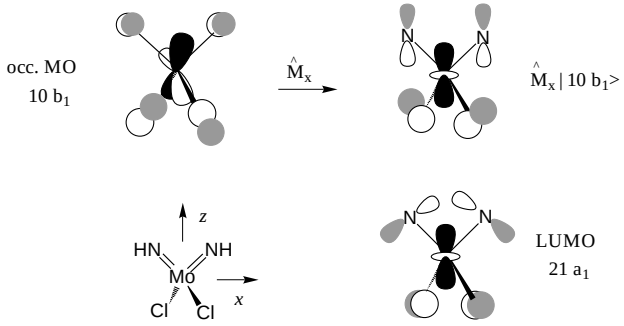

Figure 4. Schematic representations of important MOs of **12**; $\hat{M}_x$ is the angular momentum operator in the x direction.

Substituent effects: How does substitution of the two chlorine atoms in **12** affect the ^{95}Mo chemical shift of the reactant and the key barriers for metathesis? Tables 2 and 3 summarize the schematic sketch of MOs which give rise to the largest single contribution to the paramagnetic (i. e. deshielding) contribution of the magnetic shielding tensor of **12** (according to an

Table 3. Relative energies in the $[Mo(NH)_2X_2] + H_2C{=}NH$ system (kJ mol^{-1} relative to the metallacycle, BP86/AE1 level) as a function of X (labels in parentheses).

X	(metallacycle)		(**TSa**)	ΔE_a(a)	(**TSb**)	ΔE_a(b)	(Adduct **a**)		(Adduct **b**)		ΔE_{diss}[a]
Br	(**19**)	0.0	(**TS23a**)	102.5	(**TS23b**)	139.3	(**23a**)	4.0	(**23b**)	25.9	65.3
Cl[b]	(**14**)	0.0	(**TS13a**)	103.3	(**TS13b**)	136.4	(**13a**)	3.3	(**13b**)	21.7	65.7
OMe	(**20**)	0.0	(**TS24a**)	112.5	(**TS24b**)	127.6	(**24a**)	46.6	(**24b**)	41.4	68.2
OCF_3	(**21**)	0.0	(**TS25a**)	100.8	(**TS25b**)	111.3	(**25a**)	−7.4	(**25b**)	7.6	69.9
F	(**22**)	0.0	(**TS26a**)	107.9	(**TS26b**)	118.4	(**26a**)	12.3	(**26b**)	12.4	74.5

[a] Separated $[Mo(NH)_2X_2] + H_2C{=}NH$. [b] See Figure 3 for the values including zero-point corrections.

UDFT calculation with common gauge origin).[49] For this species, the principal tensor components along the x axis (following the labeling in Figure 4) is the most deshielded one ($\delta_{xx,yy,zz} = 381, -602$, and -46, respectively). Upon action of the magnetic operator in the x direction (with the same characteristics as the angular momentum operator applied in Figure 4), the high-lying occupied MO with its large d_{yz}(Mo) character is transformed into an orbital with a large d_{z^2} (Mo) contribution.[50] The latter orbital can overlap with virtual MOs that also have d_{z^2} character, such as the LUMO shown in Figure 4. The paramagnetic contribution in the x direction from these two coupled MOs, denoted $\sigma_p^{k\rightarrow a}$, as well as their energetic separation, $\Delta\varepsilon$, is included in Table 2. Even though they do not fully reflect the trend in the isotropic chemical shifts,[51] both properties appear to be related to each other, which illustrates that higher shieldings are associated with a larger separation of the important MOs.[52] As is commonly found for high-valent (d^0) compounds of early or middle transition elements, the model species $[Mo(NH)_2X_2]$ show thus "inverse halogen (or electronegativity) dependence".[53, 54]

The same ^{95}Mo chemical-shift sequence as observed for $[Mo(NH)_2X_2]$ is obtained for $[Mo(NH)_2X_2(OMe_2)]$ adducts (values in parentheses in Table 2) which serve as models for the solvated species expected to be present in the experiment. In these adducts, the ^{95}Mo nucleus appears to be deshielded by a fairly constant amount, $\approx$200 ppm, with respect to the pristine tetrahedral complexes.

The energetic data pertinent to the catalytic cycle as a function of X are collected in Table 3. The overall dissociation energy ΔE_{diss}, that is, the energetic separation between the diazametallacyclic resting state and the separated reactants (or degenerate products), increases successively with increasing electron-withdrawing capacity of X. For all derivatives studied, two transition states for the decomposition of the metallacycle, **TS19a**/**TS22a** and **TS19b**/**TS22b**, could be located, which correspond to **TS13a** and **TS13b**, respectively, in Figure 3. In general, **TSxa**, with imido and leaving imine groups *trans* to each other, is lower in energy than **TSxb**. An inspection of the corresponding barriers ΔE_a(a) and ΔE_a(b), respectively, shows that the variation in the former is much smaller than that in the latter, which is also apparent when the barriers are plotted versus the ^{95}Mo chemical shifts of the reactants (Figure 5).

The different sensitivity of ΔE_a(a) and ΔE_a(b) towards X may be rationalized in terms of a *trans* effect exerted by the substituents in the transition structure: in **TSxb**, different X are located *trans* to the leaving imine group which leads to large variations in the corresponding barrier. On the other hand, in **TSxa** the substituent *trans* to the leaving group is always an imido group, consistent with only minor variations in ΔE_a(a). The energetic difference $\Delta\Delta E_a = \Delta E_a(b) - \Delta E_a(a)$ could be taken as a measure of the destabilizing *trans* effect of X. In fact, $\Delta\Delta E_a$ decreases in the series from X = Br to F, that is, in the order of decreasing *trans* effect often encountered for these ligands.[55] Attempts to single out one particular factor responsible for this stereoelectronic effect (such as orbital interactions between fragments), however, have been unsuccessful.

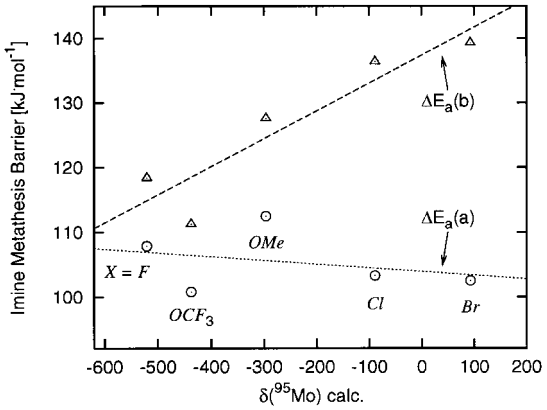

Figure 5. Correlations between computed ^{95}Mo chemical shifts and activation barriers for imine metathesis in the model system $[Mo(NH)_2X_2] + H_2C{=}NH$. ΔE_a(a) and ΔE_a(b) correspond to the paths via intermediates **TS13a** and **TS13b**, respectively, in Figure 3.

Because of the low sensitivity of the rate-determining barrier ΔE_a(a) to the substituents X, no correlation between the NMR data and the reactivity can be predicted for the set of compounds studied. So far, imine-metathetic activity has only been observed for chloro complexes and not for alkoxy derivatives,[8c] which is consistent with the larger barrier computed for the model system with X = OMe compared to that with X = Cl (Table 3, Figure 5). However, no activity has been found for fluorinated alkoxy ligands such as X = $OC(CF_3)_2(Me)$ either, whereas for the model complex with X = OCF_3 the smallest barrier is computed. Apparently, the latter substituent is not a very good model for the former. From the results in Table 3 and Figure 5 one can predict that the bromo complexes should show slightly higher catalytic activity than their chloro congeners.

If the overall trend between ΔE_a(b) and $\delta(^{95}Mo)$ would extend beyond the range covered in Figure 5, one might speculate that corresponding complexes with an even more shielded metal could in fact be associated with lower overall barriers and, thus, with a higher catalytic activity than the chloro species. If this were the case, one might consider the selection of potential target complexes based on ^{95}Mo data from the literature. For instance, because dithiocarbamate ligands, R_2NCS_2 (R_2dtc), tend to increase the shielding of $^{95}Mo^{VI}$ nuclei compared to the analogous chlorine or alkoxy derivatives,[14, 56] one could suggest that compounds containing the $[Mo(NR)_2(R'_2dtc)]$ motif may be particularly active catalysts for imine metathesis. Further experimental and theoretical studies in that direction could be rewarding. In this context it is interesting to note than a correlation between the NMR data and the reactivity is already known for $[Mo(R_2dtc)]$ complexes, namely in the oxygen-transfer reaction between $[MoO_2(R_2dtc)_2]$ and PPh_3.[2c]

Conclusion

Observed trends in ^{95}Mo chemical shifts of a number of inorganic and organometallic Mo compounds can be reproduced well by the use of "pure" density functionals, for instance at the GIAO-BPW91 level. "Hybrid" functionals,

0947-6539/99/0512-3520 $ 17.50+.50/0 *Chem. Eur. J.* **1999**, *5*, No. 12

such as the popular B3LYP combination, perform considerably worse and even fail in cases where Mo–Mo multiple bonds are present. Since B3LYP has proven to be superior for other transition-metal chemical shifts, the performance of the various functionals apparently has to be reassessed for every new problem at hand. This situation is somewhat unsatisfactory from a theoretical point of view; however, it should not prevent useful applications.

Study of the model reaction between $[Mo(NH)_2X_2]$ and $H_2C{=}NH$ confirms that the recently developed catalytic imine metathesis may proceed via intermediate Lewis adducts and diazamolybdacyclobutanes. Reversible formation and decomposition of the latter is indicated to be the rate-determining step, which can occur via two distinct transition structures with different orientation of the ligands about Mo. The lower of these two barriers occurs when the imido group is *trans* to the incoming (or leaving) imine. Upon variation of the substituents X, this rate-determining barrier is not much affected. Since the ^{95}Mo chemical shifts computed for the reactants $[Mo(NH)_2X_2]$ cover a noticeable range, no general correlation between $\delta(^{95}Mo)$ and the catalytic activities should be expected for the real imine-metathesis catalysts.

In contrast, the activation energy via the second transition state with X *trans* to the imine depends notably on X, indicative of a large stereoelectronic *trans* effect of the ligands. From the predicted loose correlation between this barrier and the ^{95}Mo chemical shifts of the reactant complexes as a function of X, one may speculate that species with particularly high ^{95}Mo shieldings could be more active than the catalysts employed so far. If confirmed experimentally, this would allow the selection of new synthetic targets based on $\delta(^{95}Mo)$ data from the literature, for instance, for imido complexes that contain dithiocarbamato ligands.

Acknowledgments

The author wishes to thank Prof. Dr. W. Thiel for his continuous support, Dr. M. Kaupp and Dipl.-Chem. N. Fröhlich for valuable suggestions, and Prof. Dr. W. von Philipsborn for his interest and for a preprint of ref. [1]. Calculations have been carried out on a Silicon Graphics PowerChallenge (Organisch-chemisches Institut, Universität Zürich) and on IBM RS6000 workstations (C4 cluster, ETH Zürich), as well as on a NEC-SX4 (CSCS, Manno, Switzerland).

[1] Review: W. von Philipsborn, *Chem. Soc. Rev.* **1999**, 95–106.
[2] See, for example: a) P. DeShong, D. R. Sidler, P. J. Rybczynski, A. A. Ogilvie, W. von Philipsborn, *J. Org. Chem.* **1989**, *54*, 5432–5437; b) M. Koller, W. von Philipsborn, *Organometallics* **1992**, *11*, 467–468; c) K. Unoura, R. Kikuchi, A. Nagasawa, Y. Kato, Y. Fukuda, *Inorg. Chim. Acta* **1995**, *228*, 89–92; d) E. J. Meier, W. Kozminski, A. Linden, P. Lustenberger, W. von Philipsborn, *Organometallics* **1996**, *15*, 2469–2477.
[3] a) H. Bönnemann, W. Brijoux, R. Brinkmann, W. Meurers, R. Mynott, W. von Philipsborn, T. Egolf, *J. Organomet. Chem.* **1984**, *272*, 231–249; b) R. Fornika, H. Görls, B. Seeman, W. Leitner, *J. Chem. Soc. Chem. Commun.* **1995**, 1479–1480.
[4] a) M. Bühl, O. L. Malkina, V. G. Malkin, *Helv. Chim. Acta* **1996**, *79*, 742–754; b) M. Bühl, *Organometallics* **1997**, *16*, 261–267.
[5] a) M. Bühl, *Angew. Chem.* **1998**, 110, 153–155; *Angew. Chem. Int. Ed.* **1998**, *37*, 142–144; b) M. Bühl in *Modeling NMR Chemical Shifts* (Eds.: J. Facelli, A. DeDios), ACS Symposium Series, *Vol. 732*, in press.
[6] T. Ziegler, *Can. J. Chem.* **1995**, *73*, 743–761.
[7] For recent reviews see: a) M. Kaupp, V. G. Malkin, O. L. Malkina in *The Encyclopedia of Computational Chemistry* (Eds.: P. von R. Schleyer, N. L. Allinger, T. Clark, J. Gasteiger, P. A. Kollman, H. F. Schaefer, III, P. R. Schreiner), Wiley, Chichester, **1998**, pp. 1857–1866; b) M. Bühl, M. Kaupp, V. G. Malkin, O. L. Malkina, *J. Comput. Chem.* **1999**, *20*, 91–105; c) G. Schreckenbach, T. Ziegler, *Theor. Chem. Acc.* **1998**, *99*, 71–82.
[8] a) G. K. Cantrell, T. Y. Meyer, *J. Chem. Soc. Chem. Commun.* **1997**, 1551–1552; b) G. K. Cantrell, T. Y. Meyer, *Organometallics* **1997**, *16*, 5381–5383; c) G. K. Cantrell, T. Y. Meyer, *J. Am. Chem. Soc.* **1998**, *120*, 8035–8042.
[9] For reviews, see: a) R. R. Schrock, *Acc. Chem. Res.* **1990**, *23*, 158–165; b) C. Pariya, K. N. Jayaprakash, A. Sarkar, *Coord. Chem. Rev.* **1998**, *168*, 1–48.
[10] See, for example: a) A. K. Rappé, W. A. Goddard, *J. Am. Chem. Soc.* **1982**, *104*, 448–456; b) E. Folga, T. Ziegler, *Organometallics* **1993**, *12*, 325–337; c) Y.-D. Wu, Z.-H. Peng, *J. Am. Chem. Soc.* **1997**, *119*, 8043–8049.
[11] M. Bühl, *Chem. Phys. Lett.* **1997**, *267*, 251–257.
[12] N. Godbout, E. Oldfield, *J. Am. Chem. Soc.* **1997**, *119*, 8065–8069.
[13] A preliminary account of these results has already been included in ref. [7b].
[14] a) M. Minelli, J. H. Enemark, R. T. C. Brownlee, M. J. O'Connor, A. G. Wedd, *Coord. Chem. Rev.* **1985**, *68*, 169–278; b) P. S. Pregosin in *Transition Metal Nuclear Magnetic Resonance* (Ed.: P. S. Pregosin), Elsevier, Amsterdam **1991**, pp. 67–81; c) J. Malito, *Ann. Rep. NMR Spectrosc.* **1997**, *33*, 151–206.
[15] A. D. Becke, *Phys. Rev. A* **1988**, *38*, 3098–3100.
[16] a) J. P. Perdew, *Phys. Rev. B* **1986**, *33*, 8822–8824; b) J. P. Perdew, *Phys. Rev. B* **1986**,*34*, 7406.
[17] D. Andrae, U. Häußermann, M. Dolg, H. Stoll, H. Preuß, *Theor. Chim. Acta* **1990**, *77*, 123–141.
[18] a) W. J. Hehre, R. Ditchfield, J. A. Pople, *J. Chem. Phys.* **1972**, *56*, 2257–2261; b) P. C. Hariharan, J. A. Pople, *Theor. Chim. Acta.* **1973**, *28*, 213–222.
[19] 6-41(d) for Se, see also: R. C. Binning, L. A. Curtiss, *J. Comput. Chem.* **1990**, *11*, 1206–1216.
[20] J. R. Cheeseman, G. W. Trucks, T. A. Keith, M. J. Frisch, *J. Chem. Phys.* **1996**, *104*, 5497–5509.
[21] a) J. J. Perdew in *Electronic Structure of Solids* (Eds.: P. Ziesche, H. Eischrig), Akademie Verlag, Berlin, **1991**; b) J. P. Perdew, Y. Wang, *Phys. Rev. B* **1992**, *45*, 13244–13249.
[22] A. D. Becke, *J. Chem. Phys.* **1993**, *98*, 5648–5642.
[23] C. Lee, W. Yang, R. G. Parr, *Phys. Rev. B* **1988**, *37*, 785–789.
[24] S. Huzinaga, M. Klobukowski, *J. Mol. Struct.* **1988**, *167*, 1–210.
[25] W. Kutzelnigg, U. Fleischer, M. Schindler in *NMR Basic Principles and Progress, Vol. 23*, Springer, Berlin, **1990**, pp. 165–262.
[26] For the Se basis set see: a) U. Fleischer, Ph. D. thesis, Universität Bochum, Germany, **1992**; b) M. Bühl, W. Thiel, U. Fleischer, W. Kutzelnigg, *J. Phys. Chem.* **1995**, *99*, 4000–4007.
[27] a) V. G. Malkin, O. L. Malkina, M. E. Casida, D. R. Salahub, *J. Am. Chem. Soc.* **1994**, *116*, 5898–5908; b) V. G. Malkin, O. L. Malkina, L. A. Eriksson, D. R. Salahub in *Modern Density Funtional Theory* (Eds.: J. M. Seminario, P. Politzer), Elsevier, Amsterdam, **1995**, pp. 273–347.
[28] M. J. Frisch, G. W. Trucks, H. B. Schlegel, P. M. W. Gill, B. G. Johnson, M. A. Robb, J. R. Cheeseman, T. Keith, G. A. Petersson, J. A. Montgomery, K. Raghavachari, M. A. Al-Laham, V. G. Zakrzewski, J. V. Ortiz, J. B. Foresman, C. Y. Peng, P. Y. Ayala, W. Chen, M. W. Wong, J. L. Andres, E. S. Replogle, R. Gomperts, R. L. Martin, D. J. Fox, J. S. Binkley, D. J. DeFrees, J. Baker, J. J. P. Stewart, M. Head-Gordon, C. Gonzales, J. A. Pople, Gaussian 94, Pittsburgh PA, **1995**.
[29] a) D. R. Salahub, R. Fournier, P. Mlynaski, I. Papai, A. St.-Amant, J. Ushio in *Density Functional Methods in Chemistry* (Eds.: J. Labanowski, J. Andzelm), Springer, New York, **1991**; b) A. St.-Amant, D. R. Salahub, *Chem. Phys. Lett.* **1990**, *169*, 387–392.
[30] For **1**, see, for example: T. J. R. Weakley, *Acta Cryst.* **1987**, *C43*, 2221–2222; for **5**: M. G. Kanatzidid, D. Coucouvanis, *Acta Crystallogr. Sect. C* **1983**, *39*, 835–838; for **6**: S. C. O'Neal, J. W: C. Olis, *J. Am. Chem.*

Soc. **1988**, *110*, 1971 – 1973; for **11**: G. A. Robbins, D. S. Martin, *Inorg. Chem.* **1984**, *23*, 2086 – 2093.
[31] M. H. Chisholm, F. A. Cotton, C. A. Murillo, W. W. Reichert, *Inorg. Chem.* **1977**, *16*, 1801 – 1808.
[32] S. P. Arnensen, H. M. Seip, *Acta Chem. Scand*. **1966**, *20*, 2711 – 2727.
[33] A GED structure is known for $[Mo_2(O_2CMe)_4]$; the Mo – Mo distance is ≈1 pm shorter than that in the solid state. See: A. H. Kelley, M. Fink, *J. Chem. Phys.* **1982**, *76*, 1407 – 1416.
[34] See also: M. R. Bray, R. J. Deeth, V. J. Paget, P. D. Sheen, *Int. J. Quantum Chem.* **1996**, *61*, 85 – 91.
[35] One referee questioned the justification of the use of DFT methods for anionic species; so far no general problems have emerged for NMR properties of related oxo anions [see, for example: a) M. Kaupp, O. L. Malkina, V. G. Malkin, *J. Chem. Phys.* **1997**, *106*, 9201 – 9212; b) G. Schreckenbach, T. Ziegler, *Int. J. Quantum Chem*. **1997**, *61*, 899 – 918]; for a performance of DFT methods for electron affinities see, for example: c) G. S. Tschumper, H. F. Schaefer, *J. Chem. Phys.* **1997**, *107*, 2529 – 2541.
[36] SOS-DFPT is UDFT together with the so-called Malkin correction (ref. [27]) which serves to reduce the paramagnetic contributions and, thus, the slope of the regression line (Table 1). While it noticeably improves the values of the chemical shifts of many lighter nuclei, the Malkin correction turns out to be relatively small for the metal shift in Mo compounds; the same has been found previously for Fe chemical shifts (ref. [4a]).
[37] H. Nakatsuji, M. Sugimoto, *Inorg. Chem*. **1990**, *29*, 1221 – 1225.
[38] J. E. Combariza, J. H. Enemark, M. Barfield, J. C. Facelli, *J. Am. Chem. Soc*. **1989**, *111*, 7619 – 7621.
[39] Part of the differences between the HF values reported here and in ref. [38] probably result from the different geometries employed (optimized versus solid-state). When the solid-state geometries are employed, GIAO-HF/II data are in fact quite close to the LORG data: the δ_{calcd} versus δ_{exp} slope for **1**, **5**, **6**, and **7** is ≈1.66, which, including **10** and **11**, is reduced to ≈0.93 and 1.18 at GIAO-BPW91 and GIAO-B3LYP, respectively.
[40] For instance, the formal sextuple bond in Cr_2 is a notorious case for ab initio methods. See, for example: a) H. Stoll, H.-J. Werner, *Mol. Phys.* **1996**, *88*, 793 – 802, and references therein; instabilities in the HF wavefunction of **11** and related species are well-known, for example: b) M. Benard, *J. Chem. Phys.* **1979**, *71*, 2546 – 2556; c) M. B. Hall, *Polyhedron* **1987**, *6*, 679 – 684.
[41] The calculation of $\delta(^{57}Fe)$ of ferrocene, on the other hand, is also a failure for GIAO-HF (and also for pure density functionals), although it was not for GIAO-B3LYP, see ref. [11].
[42] The excellent performance of the pure DFT methods for Mo compounds may to some extent be the result of error cancellation between an inherent underestimation of the paramagnetic contributions and an overestimation thereof because of the longer bonds in the optimized geometries; nevertheless, the hybrid method also performs worse when experimental geometries are employed (cf. the regression gradients of 0.93 and 1.18 for GIAO-BPW91 and GIAO-B3LYP, respectively), including the large errors for **10** and **11**.
[43] See, for example: C. Adamo, V. Barone, *Chem. Phys. Lett*. **1998**, *298*, 113 – 119.
[44] V. C. Gibson, C. Redshaw, W. Clegg, M. R. J. Elsegood, *J. Chem. Soc. Chem. Commun.* **1994**, 2635 – 2636.
[45] In order to ensure that **TS13a** and **TS13b** connect the minima shown in Figure 3, the relevant parts of the intrinsic reaction coordinate have been followed [a) C. Gonzales, H. B. Schlegel, *J. Chem. Phys.* **1989**, *90*, 2154 – 2161; b) C. Gonzales, H. B. Schlegel, *J. Phys. Chem.* **1990**, *94*, 5523 – 5527].
[46] K. Monteyne, T. Ziegler, *Organometallics* **1998**, *17*, 5901 – 5907.
[47] When heavy atoms are attached to the nucleus under scrutiny, spin-orbit effects on the chemical shifts may become important, see for example: a) M. Kaupp, O. L. Malkina, V. G. Malkin, *Chem. Phys. Lett*. **1997**, *265*, 55 – 59; for the Mo^{VI} complexes of the present study, such effects should be small because of the small s character in the bonding. See ref. [7b] and b) M. Kaupp, O. L. Malkina, V. G. Malkin, P. Pyykkö, *Chem. Eur. J.* **1998**, *4*, 118 – 126.
[48] Review: A. E. Reed, L. A. Curtiss, F. Weinhold, *Chem. Rev.* **1988**, *88*, 899 – 926.
[49] Similar total shieldings are obtained to those from distributed-gauge methods; alternatively, one could analyze the contributions in the GIAO framework; however, the Gaussian 94 program does not provide the corresponding MO analysis.
[50] For similar pictorial rationalizations of paramagnetic contributions see ref. [25] and, for example, a) Y. Ruiz-Morales, G. Schreckenbach, T. Ziegler, *J. Phys. Chem*. **1996**, *100*, 3359 – 3367; b) Y. Ruiz-Morales, T. Ziegler, *J. Phys. Chem. A* **1998**, *102*, 3970 – 3976.
[51] The shielding in **16** – **18** is dominated by a large number of other $\sigma_p^{k\rightarrow a}$ contributions not discussed here; for **18** the *x* direction is not the most deshielded one any more.
[52] Other factors may also be important, in particular the r^{-3} factors in the sum-over-states expressions which should be affected by the charges in Table 2; for a related discussion of $\delta(^{18}O)$ in transition-metal oxo complexes see ref. [35a].
[53] See, for example: a) D. Rehder, in *Transition Metal Nuclear Magnetic Resonance* (Ed.: P. S. Pregosin), Elsevier, Amsterdam, **1991**, pp. 1 – 58; b) R. G. Kidd, *Ann. Rep. NMR Spectrosc*. **1991**, *23*, 85 – 139; c) H. Nakatsuji, Z.-M. Hu, T. Nakajima, *Chem. Phys. Lett*. **1997**, *257*, 429 – 436; in some cases, inverse halogen dependence is also found for late transition metal complexes, for example: d) F. Pichierri, E. Chairparin, E. Zangrando, L. Randaccio, D. Holtenrich, B. Lippert, *Inorg. Chim. Acta* **1997**, *264*, 109 – 116.
[54] Main group nuclei usually follow the "normal halogen dependence". See, for example: R. G. Kidd, *Ann. Rep. NMR Spectrosc*. **1980**, *10A*, 1 – 79; see also ref. [47a].
[55] See, for example: a) T. G. Appleton, H. C. Clark, L. E. Manzer, *Coord. Chem. Rev.* **1973**, *10*, 335 – 422; b) M. M. Gofmann, V. I. Nefedov, *Inorg. Chim. Acta* **1978**, *28*, 1 – 17.
[56] Indeed, a sizeable shielding is computed for model complex $[Mo(NH)_2(H_2dtc)_2]$, $\delta(^{95}Mo) = -504$, although it is not more shielded than the fluoro derivative **18** (Table 2).

Received: March 15, 1999 [F 1675]

  0947-6539/99/0512-3522 $ 17.50+.50/0